Resource

Cell

Anatomical Profiling of G Protein-Coupled Receptor Expression

Jean B. Regard,[1,2,*] Isaac T. Sato,[1] and Shaun R. Coughlin[1,*]
[1]Cardiovascular Research Institute, University of California, San Francisco, San Francisco, CA 94158, USA
[2]Present address: National Institutes of Health, National Human Genome Research Institute, Building 49, Room 4C60, 49 Convent Dr., MSC 4472, Bethesda, MD 20892-4472, USA
*Correspondence: regardj@mail.nih.gov (J.B.R.), shaun.coughlin@ucsf.edu (S.R.C.)
DOI 10.1016/j.cell.2008.08.040

SUMMARY

G protein-coupled receptors (GPCRs) comprise the largest family of transmembrane signaling molecules and regulate a host of physiological and disease processes. To better understand the functions of GPCRs in vivo, we quantified transcript levels of 353 nonodorant GPCRs in 41 adult mouse tissues. Cluster analysis placed many GPCRs into anticipated anatomical and functional groups and predicted previously unidentified roles for less-studied receptors. From one such prediction, we showed that the Gpr91 ligand succinate can regulate lipolysis in white adipose tissue, suggesting that signaling by this citric acid cycle intermediate may regulate energy homeostasis. We also showed that pairwise analysis of GPCR expression across tissues may help predict drug side effects. This resource will aid studies to understand GPCR function in vivo and may assist in the identification of therapeutic targets.

INTRODUCTION

Mammalian cells sense myriad signals in their environment via G protein-coupled receptors (GPCRs), the largest family of transmembrane signaling molecules. GPCRs can be partitioned into two groups: odorant/sensory and nonodorant. Odorant/sensory receptors are restricted to specialized cells that detect external cues—odors, tastes, and pheromones—and regulate organismal behaviors such as feeding and mating. Nonodorant GPCRs are differentially expressed throughout the organism, respond to diverse endogenous ligands, and regulate a host of physiological processes including hematopoiesis, hemostasis, immune function, metabolism, neurotransmission, reproduction, cardiac function, and vascular tone. Accordingly, such receptors are the targets for about one-third of all approved drugs (Hopkins and Groom, 2002; Muller, 2000). Although in vivo roles have been defined for many of the approximately 370 nonodorant GPCRs in mice and humans, the expression and function of many such receptors are incompletely characterized, and a significant fraction remain orphans (Fredriksson et al., 2003; Fredriksson and Schioth, 2005; Hill et al., 2002; Joost and Methner, 2002; Vassilatis et al., 2003).

To support studies of nonodorant GPCR function, we analyzed the pattern of GPCR mRNA expression across tissues and the relative abundance for each of 353 nonodorant GPCRs in 41 tissues from adult mice. Hierarchical clustering analysis revealed groupings of tissues and receptors that predicted physiological functions for individual receptors and receptor clusters. We tested one such prediction by examining Gpr91, a receptor for the citric acid cycle intermediate succinate (He et al., 2004). Gpr91 was grouped in the "adipose cluster," but neither Gpr91 nor succinate was known to regulate adipocyte functions. We demonstrated that extracellular succinate can inhibit lipolysis in white adipose tissue in a manner consistent with its acting via adipocyte Gpr91. Overall, this data set provides a resource for those interested in finding previously unidentified roles for GPCRs with known ligands and hints regarding the functions of orphan GPCRs and the sources of their ligands. When compared with human expression data (SymAtlas, SAGEmap), these mouse data will aid the rational use of mice to model GPCR function in human physiology and disease and may help point up new therapeutic targets and predict on-target side effects. In addition, these quantitative data describing expression of a large number of related and relatively small genes across many tissues may support studies aimed at identifying *cis*-acting elements and transcription factors that dictate expression in particular tissues.

RESULTS

Tissue Profiling of GPCRs by qPCR

GPCRs are usually expressed at low levels. Indeed, nonodorant GPCRs comprise about 1% of genes in the genome, but only 0.001%–0.01% of expressed sequence tags (ESTs) correspond to GPCRs (Fredriksson and Schioth, 2005). Accordingly, we chose TaqMan-type quantitative real-time polymerase chain reaction (qPCR) for its high sensitivity, specificity, and broad dynamic range to measure GPCR mRNA expression. Primer/probe sets were validated as described in the Experimental Procedures; their sequences are provided in Table S3 available online.

Transcript levels for 353 GPCRs were profiled in 41 adult tissues isolated from C57BL/6 mice. Bar graphs indicating transcript levels for each receptor in each tissue relative to internal controls (β-actin, cyclophilin, GAPDH, and ribosomal protein S9) are found in the Supplemental Data Set and at http://pdsp.med.unc.edu/apGPCRe/.

Table 1. GPCRs Ubiquitously and Abundantly Expressed In Vivo

Tissue	GPCRs
Ubiquitous	Cd97, Ebi2, Edg1(S1p1), Edg3(S1p3), Ednra, Etl(Eltd1), F2r(Par1), Fzd1, Fzd7, Gabbr1, Gpr10(Prlhr), Gpr105(P2ry14), Gpr107, Gpr108, Gpr19, Gpr56, Il8rb(Cxcr2), Lec1(Lphn2), Lec2(Lphn1), P2y5, Ptger1(Ep1), Tm7sf1(Gpr137b), Tm7sf1l1(Gpr137), Tm7sf3, Tpra40(Gpr175)
CNS	Adcyap1r1, Adora1, Bai1, Bai2, Celsr2, Chrm1, Cnr1, Drd1, Drd4, Edg1(S1p1), Ednrb, Fy(Darc), Fzd1, Fzd3, Gabbr1, Glp2r, Gpr108, Gpr22, Gpr26, Gpr37(Paelr), Gpr37l1, Gpr49(Lgr5), Gpr51(Gabbr2), Gpr56, Gprc5b(Raig2), Grca(Gpr162), Grm1(Mglur1), Grm3(Mglur3), Grm4(Mglur4), Grm5(Mglur5), Grm6(Mglur6), Grm7(Mglur7), Hrh3, Il8rb(Cxcr2), Kiaa1828(Gpr123), Lec2(Lphn1), Lec3(Lphn3), Ntsr2, Opn1mw, Opn1sw, Oprl1, Pgr15(Gpr165), Pgr22(Gpr155), Rgr, Rho, Tm7sf1l1(Gpr137)
Endocrine	Adora1, Agtr1(Agtr1a), Casr, Drd2, F2r(Par1), Ghrhr, Glp1r, Gpr108, Gpr48(Lgr4), Gpr56, Lec2(Lphn1), Rai3(Gprc5a), Rdc1(Cxcr7), Tm7sf1(Gpr137b), Tm7sf1l1(Gpr137)
Cardiovascular	Agtr1(Agtr1a), Chrm2, Edg1(S1p1), Ednra, Etl(Eltd1), F2r(Par1), Fzd1, Fzd2, Fzd4, Kiaa0758(Gpr116), Rdc1(Cxcr7)
Metabolic	Adrb3, Agtr1(Agtr1a), Cmkbr1l1(Ccr1l1), Edg1(S1p1), Etl(Eltd1), Fzd4, Gcgr, Gpr10(Prlhr), Gpr48(Lgr4), Gpr56, Gpr91(Sucnr1), Hm74(Gpr109a), Ptger3(Ep3), Pthr1, Tm7sf1(Gpr137b)
Gastroenteric	Cckar, Flj14454(Gpr128), Fzd1, Glp1r, Gpr108, Ptger3(Ep3), Rai3(Gprc5a)
Immune	Adrb2, Ccr9, Cxcr4, Edg1(S1p1), Fpr-rs2, Gpr18, Il8rb(Cxcr2), Mrga3, P2y5
Reproductive	Agtr1(Agtr1a), Gpcr150, Gpr108, Gpr19, Tm7sf1l1(Gpr137)
Pulmonary	Adrb2, Calcrl, Cckar, Cd97, Edg1(S1p1), Edg3(S1p3), Etl(Eltd1), F2r(Par1), Glp1r, Gpr108, Gpr56, Kiaa0758(Gpr116), Rai3(Gprc5a), Tm7sf1(Gpr137b), Tm7sf1l1(Gpr137)
Barrier	Hm74(Gpr109a)

GPCR expression levels varied dramatically by tissue. Predictably, rhodopsin was the most abundantly expressed GPCR and among the most tissue specific, present at ~350,000 arbitrary units (a.u.) in eye but below 25 a.u. in other tissues (see below). Because rhodopsin presumably serves no function in extraocular tissues, we adopted the convention that receptors with expression values below 25 a.u. in a given tissue were "absent." With this criterion, only 25 GPCRs were expressed above background in all 41 tissues assayed (Table 1); 90 were expressed in greater than half of tissues and 238 in less than half (Figure 1A). Some ubiquitously expressed GPCRs were highly expressed in blood vessels [i.e., *Edg1(S1p1)*, *F2r(Par1)*, *Ednra*, *Ptger1*], perhaps accounting for their presence in all tissues (Table 1). Other ubiquitously expressed receptors, including Gpr56, Lec1(Lphn2), Lec2(Lphn1), Gpr107, Gpr108, Tm7sf1(Gpr137b), Tm7sf1l1(Gpr137), Tm7sf3, and Tpra40(Gpr175), were expressed in five of five different nonvascular cell lines tested and may indeed be expressed by most cell types in vivo (Table 1 and data not shown).

Save rhodopsin, nearly all GPCRs were expressed at levels below 10,000 a.u. To provide an overview of GPCR distribution, we designated receptors expressed at 25–250, 250–2500, and >2500 a.u. as low, medium, and high expressors, respectively, and we grouped tissues by system (e.g., central nervous system [CNS], endocrine, cardiovascular, pulmonary, metabolic, gastrointestinal, immune, reproductive, and cutaneous/barrier) (Figure 1B). By these criteria, 15 or fewer receptors were expressed at high level in any tissue group but CNS.

As expected, receptors that were highly expressed in a given tissue included receptors established to play an important role in that tissue (Table 1). For example, light-detecting opsins were highly expressed in eye, and dopamine, gamma-aminobutyric acid (GABA), and glutamate receptors were highly expressed in CNS (Table 1 and Figure 2A). In endocrine tissues, the extracellular calcium-sensing receptor (Casr), which regulates parathyroid hormone secretion (Ho et al., 1995), was highly expressed in parathyroid/thyroid; the growth hormone-releasing hormone receptor (Ghrhr), which regulates growth hormone secretion (Lin et al., 1993), was high in pituitary; and the glucagon-like peptide receptor 1 (Glp1r), which regulates insulin secretion (Scrocchi et al., 1996), was high in islets (Table 1, Figure 2B, and the Supplemental Data Set). The β3 adrenergic receptor (Adrb3) and the niacin/ketone body receptor Hm74(Gpr109A) (Susulic et al., 1995; Tunaru et al., 2003), which regulate lipolysis, were among the most highly expressed receptors in adipose tissue (Table 1 and see below). Glucagon receptor (Gcgr), an important regulator of glucose homeostasis (Gelling et al., 2003), was highly expressed in liver, and the parathyroid hormone receptor (Pthr1), which regulates calcium and phosphate levels and modulates the activity of 25-hydroxyvitamin D 1-hydroxylase (Amizuka et al., 1997), was highly expressed in kidney (Table 1 and Figure 2C). In heart and blood vessels, angiotensin type 1a receptor (Agtr1), which regulates vascular tone (Ito et al., 1995; Sugaya et al., 1995), thrombin receptor (F2r; Par1) and sphingosine-1-phosphate receptor (Edg1; S1p1), which play important roles in vascular development (Connolly et al., 1996; Liu et al., 2000), and the M2 muscarinic acetylcholine receptor (Chrm2), which regulates heart rate (Gomeza et al., 1999) (Table 1 and Figure 2D), were all highly expressed. Ccr9, Cxcr4, and Il8rb(Cxcr2), which regulate leukocyte formation and function (Nagasawa et al., 1996; Shuster et al., 1995; Wurbel et al., 2001), were abundant in immune tissues (Table 1). Taken together, these results provided confidence that high-level expression in specific tissues and tissue clusters correlates with physiological function and might predict roles for less-well-characterized receptors.

Hierarchical Clustering of GPCR Expression

GPCR qPCR results were analyzed by unsupervised, hierarchical clustering to further explore potential relationships between receptor expression and tissue function. The resulting dendograms

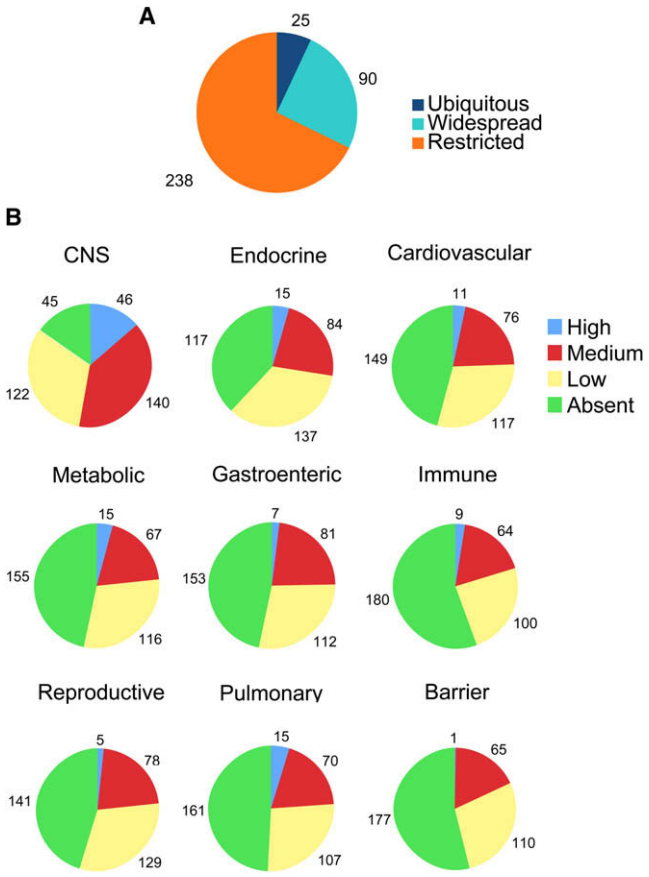

Figure 1. Distribution of Mouse GPCR mRNA Expression In Vivo

(A) The number of GPCRs expressed in tissues presented in pie chart form. Receptors expressed in all 41 tissues assayed are "ubiquitous"; receptors expressed in more than or less than half are "widespread" or "restricted," respectively. A list of the "ubiquitous" receptors is included in Table 1.

(B) GPCR expression by tissue systems. High, medium, low, and absent are defined in the Results. Tissue systems are defined as central nervous system (CNS: cerebellum, brainstem, hypothalamus, cerebral cortex, hippocampus, striatum, olfactory bulb, olfactory epithelium, retina, whole eye), endocrine (pituitary gland, islets of Langerhans, adrenal gland, thyroid/parathyroid), cardiovascular (aorta, vena cava, heart atrium, heart ventricle), pulmonary (lung, trachea), metabolic (brown adipose tissue, white adipose tissue, isolated adipocytes, liver, skeletal muscle, kidney), gastroenteric (pancreas, gall bladder, large intestine, small intestine, stomach, urinary bladder), reproductive (ovary, testes, uterus), barrier (tongue, esophagus, skin), and immune (spleen, thymus, bone marrow). A list of the highly expressed GPCRs in individual tissue systems is included in Table 1.

for both the tissue and receptor axes showed functional clusters (Figure 3A for a thumbnail image and Figure S2 for a full-size form). CNS tissues cerebellum, brainstem, hypothalamus, cerebral cortex, hippocampus, striatum, olfactory bulb, retina, and whole eye clustered together, as did the immune/hematopoietic tissues spleen, thymus, and bone marrow. The steroidogenic organs adrenal gland and ovary clustered, but testes showed a very distinct pattern of GPCR expression. Liver, kidney, and gall bladder formed a group, as did large intestine, small intestine, pancreas, and stomach. Skin, esophagus, and tongue also formed a cluster, perhaps related to their common barrier function. Cardiac atrium and ventricle, skeletal muscle, aorta, and urinary bladder formed a cluster, perhaps in part because of their sharing a relative abundance of muscle cells. Brown adipose tissue (BAT), white adipose tissue (WAT), isolated adipocytes, and vena cava formed an "adipose" cluster. The presence of vena cava in this cluster likely represents the incomplete removal of surrounding fat from the samples.

A number of receptor axis clusters were easily recognized (Figure 3). A portion of the "immune/hematopoietic" cluster is shown in Figure 3B. Included are Ccr9, Cxcr6, Cxcr4, Ccr3, Ccxcr1(Xcr1), Blr1, Pgr16(Emr4), Gpr33, Ccr6, Gpr65(Tdag8), Cnr2, Edg6(S1p4), Gpr9(Cxcr3), Ccr7, Fksg79(Gpr174), G2a(Gpr132), P2Y10, Pgr27(Gpr114), Ebi2, Gpr18, and H963(Gpr171). Most of these receptors are known to be expressed in and/or to play a role in immune cells (Birkenbach et al., 1993; Forster et al., 1996, 1999; Humbles et al., 2004; Karsak et al., 2007; Kim et al., 2001; Le et al., 2001; Malone et al., 2004; Nagasawa et al., 1996; Rao et al., 1999; Soto et al., 1998; Stacey et al., 2002; Varona et al., 2001; Wurbel et al., 2001), but no role for Fksg79(Gpr174), Pgr27(Gpr114), and H963(Gpr171) in this context has been described.

The pituitary cluster (Figure 3C) includes Bdkrb2, Gpr30(Gper), Ghrhr, Gnrhr, Drd3, Mc3r, Sstr5, Gpr2(Ccr10), and Hcrtr1(Ox1r); among these, Gpr2(Ccr10) has not been previously implicated in pituitary gland function (Brailoiu et al., 2007; Date et al., 2000; Kumar et al., 1997; Lin et al., 1993; Lorsignol et al., 1999; Tsutsumi et al., 1992).

The CNS cluster was by far the largest. Our analysis (Figure 1B and Figure 3), as well as others (Vassilatis et al., 2003), suggests that more than 80% of all nonodorant GPCRs are expressed in CNS. In Figure 3D, we show a small portion of the CNS cluster that includes Gpr101, Hcrtr2(Ox2r), Oprk1, Gpr83, Ntsr1, Gpr45, Htr1a, Htr7, Oprm1, and Npy5r, all of which have been implicated in regulation of neuronal function (Bates et al., 2006; Filliol et al., 2000; Lovenberg et al., 1993; Marsh et al., 1998; Mazella et al., 1996; Popova et al., 2007; Simonin et al., 1995; Willie et al., 2003).

Finally, Figure 3E shows the "eye/retina" cluster, which contains Glp2r, Drd4, Grm6(Mglur6), Opn1mw, Opn1sw, Pgr5(Gpr152), Rho, Rrh, Vlgr1(Gpr98), Oa1(Gpr143), and Rgr. Save Glp2r and Pgr5(Gpr152), all are known to function in the eye (Chen et al., 2001; Chiu et al., 1994; Cohen et al., 1992; Dryja et al., 2005; Incerti et al., 2000; McGee et al., 2006; Nathans and Hogness, 1983; Sun et al., 1997a, 1997b).

Taken together, the results outlined above reveal that tissues cluster into largely expected functional groups purely on the basis of their GPCR repertoires, and both expected and unique groups of receptors cluster by tissue function. These data identify sets of receptors involved in specific aspects of physiology and should prove useful in providing clues regarding in vivo roles for orphan GPCRs and new roles for receptors with known ligands. To test the latter prediction, we sought a possible role for a recently deorphanized receptor, Gpr91, found in the adipose cluster.

Extracellular Succinate Inhibits Lipolysis, Likely via Gpr91

Thirteen GPCRs defined an adipose cluster (Figure 4A and circled area in Figure 3A): Gpr64(He6), Hm74(Gpr109a), Adrb3, Gpr81, Pgr4(Gpr120), Gpr23(Lpa4), Tshr, Opn3, Oxtr, Sctr, Gpr91(Suncr1), Pthr1, and Ptger3(Ep3). Ligands for most of

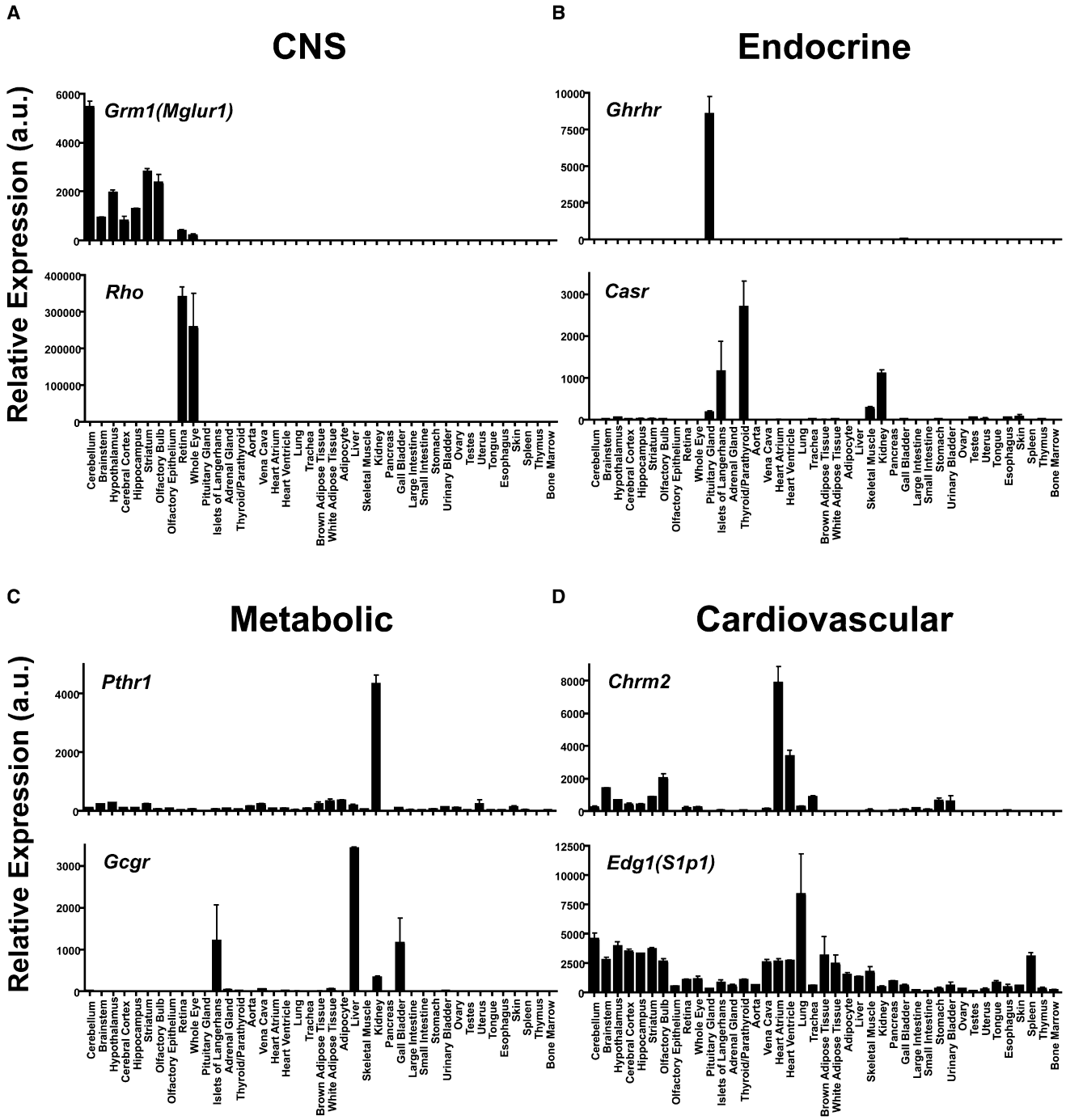

Figure 2. qRT-PCR Tissue Distribution Yields Predicted Patterns of Expression

Representative GPCRs that were highly expressed in distinct tissue systems were selected from Figure 1B and Table 1 to illustrate tissue specificity, range of expression levels, and reproducibility. Examples are shown for the following: CNS: metabotropic glutamate receptor 1 [Grm1(Mglur1)] and rhodopsin [Rho] (A); endocrine system: growth hormone releasing hormone receptor [Ghrhr] and the extracellular calcium-sensing receptor [Casr] (B); metabolic tissues: parathyroid hormone receptor 1 [Pthr1] and glucagon receptor [Gcgr] (C); and cardiovascular system: M2 muscarinic receptor [Chrm2] and the sphingosine-1-phosphate receptor 1 [Edg1(S1p1)] (D). Values are plotted as the mean ± SEM; n = 2–5.

these receptors are known to affect adipocyte function (Butcher and Carlson, 1970; Gotoh et al., 2007; Moskowitz and Fain, 1969; Rodbell, 1964; Sinha et al., 1976; Susulic et al., 1995; Tunaru et al., 2003; Valet et al., 1998), but, to our knowledge, no role for Gpr64(He6), Gpr81, Opn3, or Gpr91(Suncr1) in adipose tissue has been reported. He et al. demonstrated that the citric acid cycle

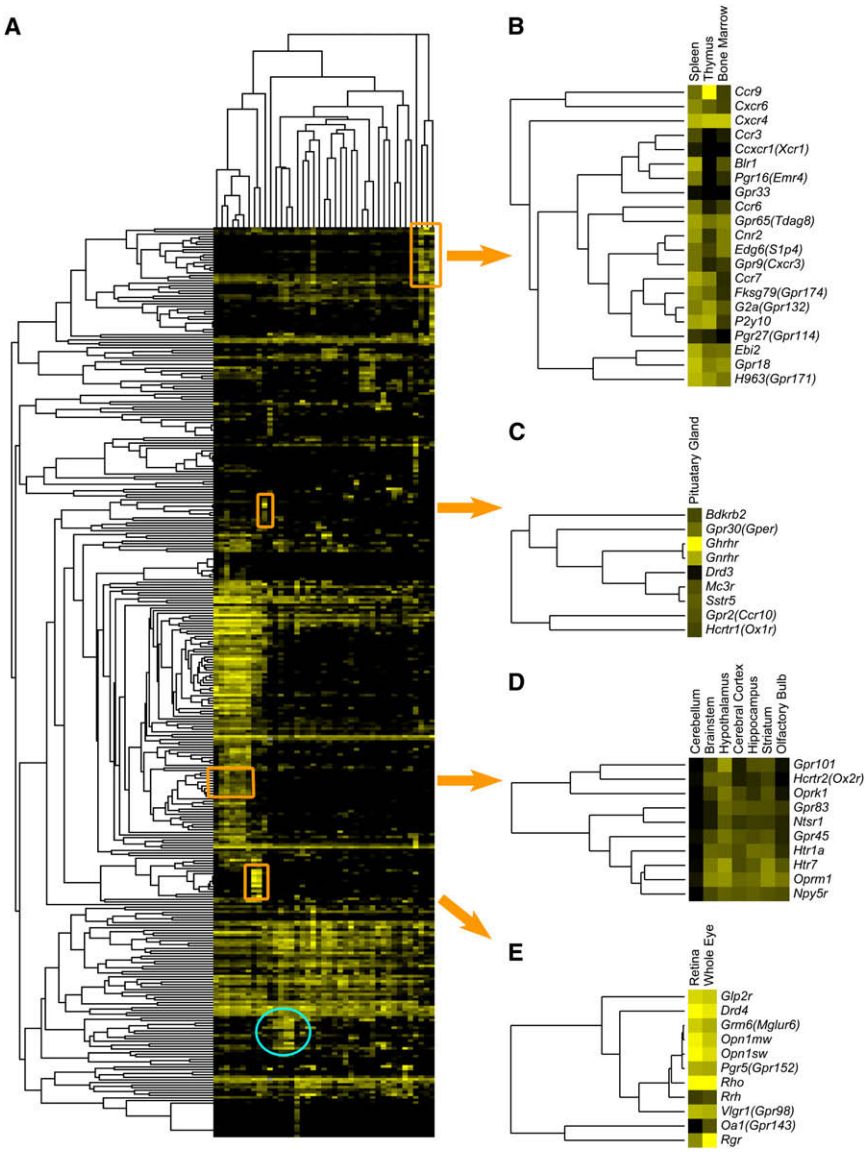

Figure 3. Unsupervised Hierarchical Clustering of GPCR Expression across Tissues

(A) Transformed qRT-PCR data for the 353 GPCRs assayed in the 41 tissues was evaluated by unsupervised hierarchical clustering with average linkage with Cluster 3.0 and visualized with Java TreeView (see the Experimental Procedures). A thumbnail image is shown here; a full-size version is shown in Figure S2. Multiple clusters and subclusters were seen, and five were chosen for further analysis. The fifth cluster (blue circle toward the bottom) is discussed in Figure 4.

(B) A portion of the "immune/hematopoietic" cluster is shown; note the abundance of chemokine receptors.

(C) The "pituitary" cluster contains many well-documented regulators of pituitary function, including Ghrhr and Gnrhr.

(D) A small portion of the "CNS" cluster, by far the largest. This portion contains receptors for important neurotransmitters including serotonin, neuropeptide Y, orexin and opiates.

(E) The "eye/retinal" cluster contains light-sensing opsins as well as other receptors known to regulate vision.

intermediate succinate can activate Gpr91 and that Gpr91, presumably in kidney, mediates elevation of plasma renin levels and blood pressure in response to exogenous succinate (He et al., 2004). Like *Adrb3* and *Hm74(Gpr109a)*, *Gpr91(Suncr1)* mRNA was most highly expressed in white adipose tissue (WAT) and was abundant in purified adipocytes (Figure 4B). Gpr91 is at least partially G_i coupled (He et al., 2004), and G_i-coupled GPCRs are known to inhibit lipolysis in adipose tissues (Moreno et al., 1983). Accordingly, we examined the effect of succinate on isoproterenol-induced lipolysis in isolated WAT (Isoproterenol has relatively low affinity for Adrb3 and most likely acts via Adrb2 in this context).

Succinate inhibited lipolysis in a dose-dependent manner with an apparent IC_{50} of 44 μM (Figure 4C), a concentration similar to the EC_{50} for succinate activation of Gpr91 heterologously expressed in 293 cells (He et al., 2004). Inhibition of lipolysis by succinate was ablated by pertussis toxin pretreatment. 3T3-L1 adipocyte-like cells, which do not express *Gpr91* mRNA (J.B.R. and S.R.C., unpublished data) and were not sensitive to the antilipolytic effects of succinate, became succinate sensitive when transfected with a mammalian expression vector for GPR91 (Figure 4E). These data strongly suggest that succinate inhibits lipolysis in WAT via a G_i-coupled GPCR, presumably Gpr91.

Pairwise Analysis of GPCR Coexpression May Help Identify Multiple Roles for Individual GPCRs

To explore whether coexpression of GPCRs might provide additional clues to function, we compared the expression pattern of each GPCR to that of every other to generate the map shown in Figure 5. Positive and negative correlation of expression patterns are indicated by yellow and blue colors, respectively (Figure 5A and Figure S3). Such correlation maps are a powerful tool for organizing and analyzing gene-gene and protein-protein interactions on a global scale (Collins et al., 2007a, 2007b; Krogan et al., 2006; Schuldiner et al., 2005; Segre et al., 2005).

Not surprisingly, tissue-specific receptor clusters similar to those seen in Figure 3 were, for the most part, recapitulated as distinct blocks along the diagonal. Examples are shown in Figures 5B, 5C, and 5D which largely reproduce the immune/hematopoietic, eye/retina, and adipose clusters of Figures 3B, 3E, and 4A, respectively. Off-diagonal blocks drew attention to possible roles for receptors in other contexts. By pointing out possible roles for receptors outside of their main physiological cluster, such analysis may be useful in understanding and predicting on-target drug side effects (see the Discussion).

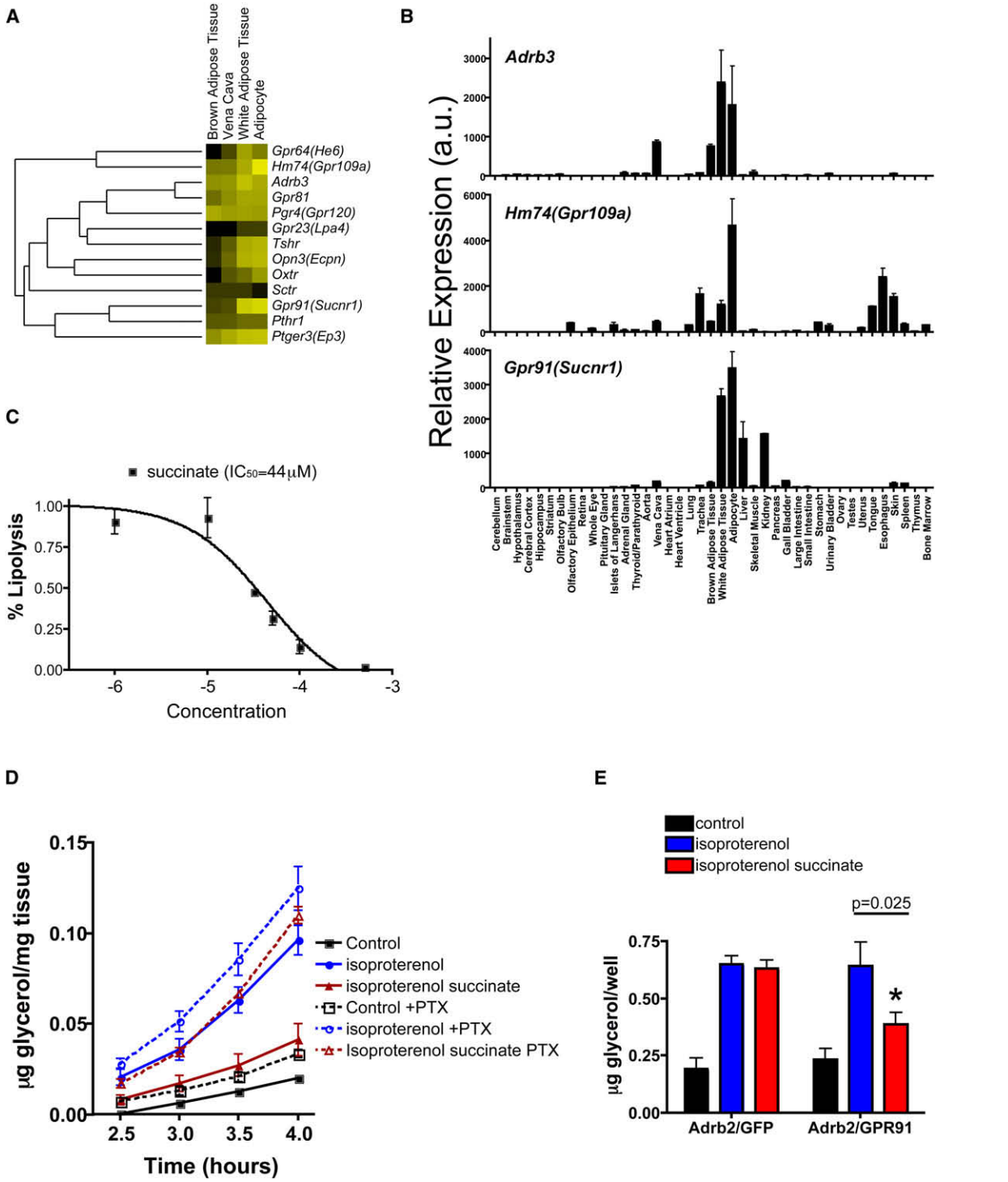

Figure 4. *Gpr91(Sucnr1)* and Its Ligand, Succinate, can Inhibit Lipolysis in Adipocytes

(A) The "adipose" cluster (blue circle, lower part Figure 3A) contained numerous regulators of adipocyte function.

(B) *Adrb3*, *Hm74(Gpr109a)* and *Gpr91(Sucnr1)* were expressed at similarly high levels in white adipose tissues (WAT) and isolated adipocytes.

(C) Isolated WAT was treated with isoproterenol (20 nM) to stimulate lipolysis, as measured by glycerol release at 3 hr. Succinate added concurrently with isoproterenol inhibited lipolysis in a concentration-dependent manner with an apparent IC_{50} of approximately 44 μM.

(D) Isolated WAT was pretreated either with KRH/BSA or KRH/BSA containing pertussis toxin (PTX; 100 ng/mL) for 3 hr prior to exposure to the indicated conditions. Isoproterenol (20 nM) -stimulated glycerol release was inhibited by the addition of 80 μM succinate. Pretreatment of WAT with PTX abrogated this effect, suggesting succinate's inhibition of lipolysis occurred in a $G_{i/o}$-dependent manner, consistent with Gpr91 activation.

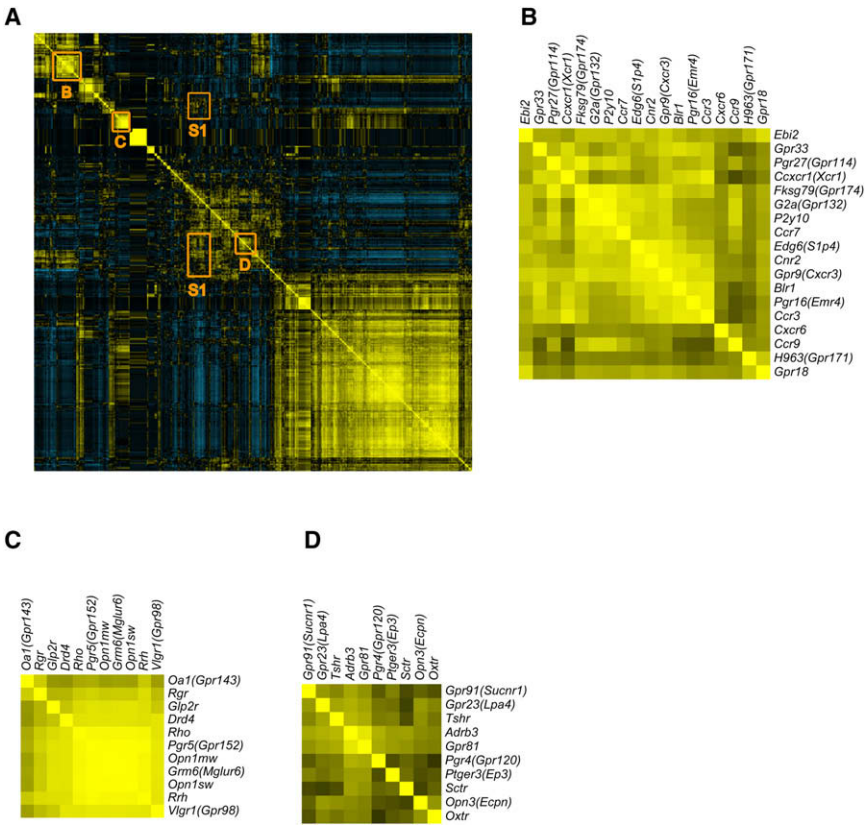

Figure 5. Hierarchical-Cluster Analysis of Pairwise GPCR Expression Reveals Additional Levels of Interaction

(A) Pearson correlation r coefficients were calculated for interactions between each GPCR with all others on the basis of tissue expression patterns. The resulting data set was further analyzed with Cluster 3.0 with complete linkage and visualized with TreeView. A thumbnail image is shown here, and a full-size image is available in Figure S3. Receptors with similar distributions are shown in yellow; distinct distributions are shown in blue. The x and y axes are mirror images of one another. The diagonal represents each receptor interacting with itself (perfect similarity in distribution).

(B–D) Clustering of receptors by similarity of expression reveals an immune/hematopoietic grouping very similar to that in Figure 3B (B), an eye/retinal cluster similar to that in Figure 3E (C), and an adipose cluster similar to that in Figure 4A (D). However, analysis of GPCR interaction clusters off the diagonal suggested receptor functions outside of their most obvious physiological roles. This might aid in understanding and prediction of on-target drug side effects (see the Discussion and Figure S1).

DISCUSSION

We have quantitated mRNA levels for the nonodorant G protein-coupled receptors encoded in the mouse genome in 41 tissues and provide this data set as a resource for predicting roles for incompletely characterized GPCRs, exploring tissue-specific gene expression, and other purposes. The fact that tissues that comprise classical physiological systems (cardiovascular, gastrointestinal, etc.) were clustered together simply on the basis of their GPCR repertoires speaks to the key roles that GPCRs play in homeostatic regulation.

Our anatomic expression profiling yielded a large amount of information consistent with known physiology, and high-level expression of a GPCR in a particular tissue cluster or specific tissue correlated well with its physiological role. Although this result is not surprising, it does provide confidence that roles for orphan receptors or GPCRs not known to play a role in a particular physiological process might be predicted by presence in a given cluster. Our demonstration that Gpr91 expression pointed to a role for extracellular succinate in regulating lipolysis in adipocytes validates this notion and is also of intrinsic interest.

The concentration of succinate in plasma has been reported at 5–125 μM, a range that surrounds the EC_{50} for Gpr91 activation (He et al., 2004) and the IC_{50} for inhibition of lipolysis in WAT (Figure 4). Succinate concentrations increase during exercise and metabolic acidosis and, in rodents, in hyperglycemic metabolic states (Forni et al., 2005; Hochachka and Dressendorfer, 1976; Krebs, 1950; Kushnir et al., 2001; Nordmann and Nordmann, 1961; Sadagopan et al., 2007). Thus, excursions in the levels of extracellular succinate do occur and might regulate adipocyte function in vivo. Adipocyte function was not investigated in mice lacking Gpr91, which are grossly healthy (He et al., 2004). Overall, a physiological role for succinate in regulating adipocyte metabolism is plausible, but when and how such a system might be important and/or redundant with other systems that govern adipocyte function remains unknown.

Forty-nine of the 353 GPCRs profiled were expressed in only one or two of the 41 tissues examined (see Table S1). Such confined expression might point out targets of pharmaceutical interest. For example, testes showed a GPCR expression pattern very distinct from that of other tissues. Gpr150, Gpr66, Gpr15, Mtnr1a, and Pgr23 were almost perfectly specific to testes. Whether such receptors play a role in spermatogenesis or other testicular functions and their potential utility as targets for drugs aimed at controlling fertility is unknown.

A comparison of each receptor's expression pattern with that of every other (Figure 5) provided a means of pointing out possible roles for a given receptor outside its main physiological cluster.

(E) Differentiated 3T3-L1 cells, which do not express *Gpr91* mRNA, were transfected with mammalian expression vectors containing β2 adrenergic receptor (Adrb2) and control (green fluorescent protein; GFP) or Adrb2 and GPR91. Succinate (100 μM) inhibited isoproterenol (10 nM) -induced lipolysis in cells cotransfected with GPR91 but not GFP. The data shown are mean ± SD, n = 3; p = 0.025, unpaired student's t test. This experiment was done three times with similar results.

Hm74(Gpr109a), the ketone body receptor that is activated therapeutically by niacin to treat dyslipidemias (Soga et al., 2003; Tunaru et al., 2003; Wise et al., 2003), provides an interesting example. By traditional clustering analysis, Hm74(Gpr109a) is placed in the "adipose" cluster (Figure 4A), and activation of adipocyte Hm74 likely mediates the antilipolytic actions of niacin (Tunaru et al., 2003). It was recently shown that the skin-flushing side effect of niacin (Carlson, 2005) is mediated by Hm74 expression by bone-marrow-derived epidermal Langerhans cells that release of vasodilatory prostanoids (Benyo et al., 2006; Benyo et al., 2005). By quantitative profiling across tissues, Hm74 was noted to be expressed relatively highly in skin and other "barrier-cluster" tissues as well as adipose (Figure 4B). By expression correlation analysis, Hm74 was not found with the adipose cluster on the diagonal but instead clustered with receptors with more widespread expression (Figures S1 and S3). A search of off-diagonal interactions revealed that Hm74 interacts not only with the adipose cluster but also with receptors in both immune and barrier clusters (Figure S1 and S3). Thus, analysis of GPCR expression data from these different perspectives may generate hypotheses regarding on-target side effects of drugs.

GPCR genes are usually relatively small, often intronless, and range from closely to distantly related. These features, plus the availability of quantitative expression data across multiple tissues for hundreds of related genes that show clusters based on shared tissue-specific patterns, may provide a resource for those interested in identifying the combinations of *cis*-acting elements that specify gene expression in a given cell type.

Some GPCRs are thought to function as heterodimers, and cluster analysis for coexpression might point to potential receptor pairs. For example, Gabbr1 is currently thought to function as an obligate heterodimer with Gpr51(Gabbr2) (Jones et al., 1998; Kaupmann et al., 1998; Kuner et al., 1999; White et al., 1998). Our data (Supplemental Data Set) and those of others (Calver et al., 2000) demonstrate similar expression patterns for these receptors in CNS and divergent expression in the periphery. These results are consistent with Gabbr1 and Gabbr2 heterodimer formation in the CNS but raise the possibility that in the periphery, expression of one or the other partner is regulated, that these receptors may use other partners, and/or that heterodimerization may not be required in all settings (Cheng et al., 2007).

Several caveats should be stated regarding interpreting our expression data. (1) Relative mRNA levels, of course, will not always reflect relative protein expression levels or the relative importance of a particular receptor in a particular tissue. Indeed, some important receptors such as adrenergic receptors were expressed at relatively low levels. (2) Tissues are comprised of multiple cell types, and receptor expression can be restricted to a minority cell type. In the extreme, receptor expression in a minority population can be missed by whole-tissue analysis. For example, neither our qPCR data (Supplemental Data Set) nor those of others (Liberles and Buck, 2006) detected trace amine associated receptor 1 (Taar1) expression in brain, but a Taar 1 Lac-Z knockin mouse revealed Taar1 expression in discrete neuronal populations and Taar1-dependent regulation of dopaminergic activity (Lindemann et al., 2008). (3) The presence of a receptor within a particular anatomical cluster does not exclude important functions in tissues outside that cluster. For example, the D2 dopamine receptor (Drd2) is recognized as the major dopamine receptor subtype in pituitary (Kelly et al., 1997; Saiardi et al., 1997), but Drd2 was in the CNS cluster, whereas the D3 dopamine receptor (Drd3) was in the pituitary cluster (Figure 3C). The cluster analysis presented here used the Pearson correlation, which normalizes expression levels (see the Experimental Procedures) to focus on gaining information from the pattern of gene expression at the cost of ignoring absolute levels of receptor expression, and the Drd cluster results are presumably a result of the fact that Drd2 is expressed at moderate levels in numerous CNS structures whereas Drd3 is expressed at very low levels in only a few structures (Supplemental Data Set). However, our quantitative expression data (Supplemental Data Set) reveal that Drd2 is expressed approximately 100-fold higher than Drd3 in pituitary, consistent with the dominant role of Drd2 in pituitary function. Thus, this resource is best utilized when the data are analyzed from several perspectives and should be viewed as a means of generating hypotheses to be tested experimentally. Raw expression data for the 353 GPCRs in the 41 organ samples are available at http://pdsp.med.unc.edu/apGPCRe/, for those who wish to perform their own analyses.

Lastly, expression of individual GPCRs in specific tissues can be different in human and mouse. When used together with GPCR expression patterns in human (SymAtlas, SAGEmap), our data set should facilitate rational use of mouse to model the roles of GPCRs in human physiology and disease.

EXPERIMENTAL PROCEDURES

qRT-PCR

Ten-week-old C56BL/6 mice (Jackson Labs) were housed in University of California, San Francisco (UCSF) animal facilities for 2 weeks prior to organ harvest. Mice were anesthetized with ketamine/xylazine and transcardially-perfused with saline for the removal of blood. Organs were dissected, rapidly frozen in liquid nitrogen, and stored at −80°C until the time of RNA isolation. Corresponding organs from two male and two female mice were pooled to yield a single tissue RNA sample (i.e., for each separate replicate, organs of four mice were pooled), with the exception of sex-specific organs, which were pooled from two mice. Pancreas was removed and stored for 24 hr in RNAlater at 4°C prior to storage at −80°C. Islets of Langerhans were isolated from 20 male C57BL/6 males by the UCSF islet isolation core. Primary adipocytes were isolated from sex organ fat pads as described (Rodbell, 1964). Tissues were first homogenized, and crude RNA was extracted with Trizol (Invitrogen). RNA was further purified with RNeasy columns (QIAGEN) with on-column DNase I digestion. RNA samples were treated with DNase I a second time and concentrated with the Zymo Research DNA-free RNA kit. First-strand synthesis was performed with the iScript kit (Biorad). qPCR assays were performed in a 384-well format with an ABI7900HT, Platinum qPCR mix (Invitrogen) and 10 μl reactions. Cycle threshold (Ct) values were collected at 0.2 for all samples; Ct values for individual GPCRs were compared to Ct values for four internal controls (β-actin, cyclophilin, GAPDH, and ribosomal protein S9) for all tissues. Taqman primer/probes have been described (Regard et al., 2007), and sequences are available in Table S3. There were 22 mouse GPCRs for which we were unable to generate primer/probe sets that produced a signal above background in any tissue. A lack of data should be viewed as "no data" for these receptors, which are listed in Table S2. PCR efficiencies were calculated as described (Peirson et al., 2003). $2^{(CtGPCR\ -\ Ctcontrol)}$ multiplied by 2^{15} was used for graphical representation of qPCR data. Repeated qPCR analysis of a given tissue RNA sample, i.e., technical replicates, yielded variations of less than 10%. Two to five independently prepared RNA samples from separate tissue isolations were analyzed for assessment of in vivo expression

variability, which was also generally less than 10%. Data presented in the Supplemental Data Set and elsewhere represent the mean ± SEM (n = 2–5).

Lipolysis

C57BL6 mice were euthanized by cervical dislocation. Sex organ fat pads were dissected and finely minced and washed four times with Krebs-Ringer HEPES buffer containing 4% fatty-acid-free bovine serum albumin (BSA), 5 mM glucose, and 0.1 mM ascorbic acid (KRH-BSA). Twenty-five to 30 milligrams of WAT mincate was placed in the upper well of transwells in a 24-well plate and placed in a tissue culture incubator at 37°C with the specified cocktail for the indicated amount of time. KRH-BSA samples were taken from the wells at the specified time for quantification of glycerol release and were divided by the weight of the mincate. Pertussis toxin (Calbiochem) pretreatment was performed for 4 hr in a tissue culture incubator with mild shaking. 3T3-L1 cells (ATCC) were cultured and differentiated via standard protocols. Fully differentiated 3T3-L1 cells were transfected (Amaxa, Nucleofection) with mammalian expression vectors containing β2-adrenergic receptor (Adrb2—generously provided by Dr. J. Silvio Gutkind) and GPR91 (Missouri S&T) and allowed to recover for 48–72 hr prior to lipolysis assays. Free glycerol was quantified with the Free Glycerol reagent (Sigma). IC_{50} for succinate inhibition of isoproterenol-induced lipolysis was calculated with Prism4.

Hierarchical Clustering

All analysis of the data was performed with Python, Scipy, and Excel. For pairwise correlation in Figure 5, Pearson correlation r values were computed between the expression vectors of every pair of genes in the data set. Transformed data were hierarchically clustered with Cluster 3.0 (Eisen et al., 1998) and visualized with Java TreeView (Saldanha, 2004).

SUPPLEMENTAL DATA

Supplemental Data include three figures, three tables, and one data set and can be found with this article online at http://www.cell.com/supplemental/S0092-8674(08)01129-X.

ACKNOWLEDGMENTS

We thank the Coughlin lab for valuable discussions, Ivo Cornelissen, Gerard Honig, and Grant Li, for technical assistance in isolating mouse tissues, and Stuart Peirson for sharing qPCR efficiency transformations. We also thank Dale Webster and Joseph Derisi for help with informatics, Silvio Gutkind for providing the Adrb2 construct, and Bryan Roth for critical reading of the manuscript. This work was supported by the National Institutes of Health (S.R.C.) and Sandler Family Foundation (J.B.R.).

Received: January 29, 2008
Revised: June 27, 2008
Accepted: August 28, 2008
Published: October 30, 2008

REFERENCES

Amizuka, N., Lee, H.S., Kwan, M.Y., Arazani, A., Warshawsky, H., Hendy, G.N., Ozawa, H., White, J.H., and Goltzman, D. (1997). Cell-specific expression of the parathyroid hormone (PTH)/PTH-related peptide receptor gene in kidney from kidney-specific and ubiquitous promoters. Endocrinology *138*, 469–481.

Bates, B., Zhang, L., Nawoschik, S., Kodangattil, S., Tseng, E., Kopsco, D., Kramer, A., Shan, Q., Taylor, N., Johnson, J., et al. (2006). Characterization of Gpr101 expression and G-protein coupling selectivity. Brain Res. *1087*, 1–14.

Benyo, Z., Gille, A., Kero, J., Csiky, M., Suchankova, M.C., Nusing, R.M., Moers, A., Pfeffer, K., and Offermanns, S. (2005). GPR109A (PUMA-G/HM74A) mediates nicotinic acid-induced flushing. J. Clin. Invest. *115*, 3634–3640.

Benyo, Z., Gille, A., Bennett, C.L., Clausen, B.E., and Offermanns, S. (2006). Nicotinic acid-induced flushing is mediated by activation of epidermal langerhans cells. Mol. Pharmacol. *70*, 1844–1849.

Birkenbach, M., Josefsen, K., Yalamanchili, R., Lenoir, G., and Kieff, E. (1993). Epstein-Barr virus-induced genes: First lymphocyte-specific G protein-coupled peptide receptors. J. Virol. *67*, 2209–2220.

Brailoiu, E., Dun, S.L., Brailoiu, G.C., Mizuo, K., Sklar, L.A., Oprea, T.I., Prossnitz, E.R., and Dun, N.J. (2007). Distribution and characterization of estrogen receptor G protein-coupled receptor 30 in the rat central nervous system. J. Endocrinol. *193*, 311–321.

Butcher, R.W., and Carlson, L.A. (1970). Effects of secretin on fat mobilizing lipolysis and cyclic AMP levels in rat adipose tissue. Acta Physiol. Scand. *79*, 559–563.

Calver, A.R., Medhurst, A.D., Robbins, M.J., Charles, K.J., Evans, M.L., Harrison, D.C., Stammers, M., Hughes, S.A., Hervieu, G., Couve, A., et al. (2000). The expression of GABA(B1) and GABA(B2) receptor subunits in the cNS differs from that in peripheral tissues. Neuroscience *100*, 155–170.

Carlson, L.A. (2005). Nicotinic acid: The broad-spectrum lipid drug. A 50th anniversary review. J. Intern. Med. *258*, 94–114.

Chen, P., Hao, W., Rife, L., Wang, X.P., Shen, D., Chen, J., Ogden, T., Van Boemel, G.B., Wu, L., Yang, M., et al. (2001). A photic visual cycle of rhodopsin regeneration is dependent on Rgr. Nat. Genet. *28*, 256–260.

Cheng, Z., Tu, C., Rodriguez, L., Chen, T.H., Dvorak, M.M., Margeta, M., Gassmann, M., Bettler, B., Shoback, D., and Chang, W. (2007). Type B gamma-aminobutyric acid receptors modulate the function of the extracellular Ca2+-sensing receptor and cell differentiation in murine growth plate chondrocytes. Endocrinology *148*, 4984–4992.

Chiu, M.I., Zack, D.J., Wang, Y., and Nathans, J. (1994). Murine and bovine blue cone pigment genes: Cloning and characterization of two new members of the S family of visual pigments. Genomics *21*, 440–443.

Cohen, A.I., Todd, R.D., Harmon, S., and O'Malley, K.L. (1992). Photoreceptors of mouse retinas possess D4 receptors coupled to adenylate cyclase. Proc. Natl. Acad. Sci. USA *89*, 12093–12097.

Collins, S.R., Kemmeren, P., Zhao, X.C., Greenblatt, J.F., Spencer, F., Holstege, F.C., Weissman, J.S., and Krogan, N.J. (2007a). Toward a comprehensive atlas of the physical interactome of Saccharomyces cerevisiae. Mol. Cell. Proteomics *6*, 439–450.

Collins, S.R., Miller, K.M., Maas, N.L., Roguev, A., Fillingham, J., Chu, C.S., Schuldiner, M., Gebbia, M., Recht, J., Shales, M., et al. (2007b). Functional dissection of protein complexes involved in yeast chromosome biology using a genetic interaction map. Nature *446*, 806–810.

Connolly, A.J., Ishihara, H., Kahn, M.L., Farese, R.V., Jr., and Coughlin, S.R. (1996). Role of the thrombin receptor in development and evidence for a second receptor. Nature *381*, 516–519.

Date, Y., Mondal, M.S., Matsukura, S., Ueta, Y., Yamashita, H., Kaiya, H., Kangawa, K., and Nakazato, M. (2000). Distribution of orexin/hypocretin in the rat median eminence and pituitary. Brain Res. Mol. Brain Res. *76*, 1–6.

Dryja, T.P., McGee, T.L., Berson, E.L., Fishman, G.A., Sandberg, M.A., Alexander, K.R., Derlacki, D.J., and Rajagopalan, A.S. (2005). Night blindness and abnormal cone electroretinogram ON responses in patients with mutations in the GRM6 gene encoding mGluR6. Proc. Natl. Acad. Sci. USA *102*, 4884–4889.

Eisen, M.B., Spellman, P.T., Brown, P.O., and Botstein, D. (1998). Cluster analysis and display of genome-wide expression patterns. Proc. Natl. Acad. Sci. USA *95*, 14863–14868.

Filliol, D., Ghozland, S., Chluba, J., Martin, M., Matthes, H.W., Simonin, F., Befort, K., Gaveriaux-Ruff, C., Dierich, A., LeMeur, M., et al. (2000). Mice deficient for delta- and mu-opioid receptors exhibit opposing alterations of emotional responses. Nat. Genet. *25*, 195–200.

Forni, L.G., McKinnon, W., Lord, G.A., Treacher, D.F., Peron, J.M., and Hilton, P.J. (2005). Circulating anions usually associated with the Krebs cycle in patients with metabolic acidosis. Crit. Care *9*, R591–R595.

Forster, R., Mattis, A.E., Kremmer, E., Wolf, E., Brem, G., and Lipp, M. (1996). A putative chemokine receptor, BLR1, directs B cell migration to defined lymphoid organs and specific anatomic compartments of the spleen. Cell *87*, 1037–1047.

Forster, R., Schubel, A., Breitfeld, D., Kremmer, E., Renner-Muller, I., Wolf, E., and Lipp, M. (1999). CCR7 coordinates the primary immune response by establishing functional microenvironments in secondary lymphoid organs. Cell *99*, 23–33.

Fredriksson, R., Lagerstrom, M.C., Lundin, L.G., and Schioth, H.B. (2003). The G-protein-coupled receptors in the human genome form five main families. Phylogenetic analysis, paralogon groups, and fingerprints. Mol. Pharmacol. *63*, 1256–1272.

Fredriksson, R., and Schioth, H.B. (2005). The repertoire of G-protein-coupled receptors in fully sequenced genomes. Mol. Pharmacol. *67*, 1414–1425.

Gelling, R.W., Du, X.Q., Dichmann, D.S., Romer, J., Huang, H., Cui, L., Obici, S., Tang, B., Holst, J.J., Fledelius, C., et al. (2003). Lower blood glucose, hyperglucagonemia, and pancreatic alpha cell hyperplasia in glucagon receptor knockout mice. Proc. Natl. Acad. Sci. USA *100*, 1438–1443.

Gomeza, J., Shannon, H., Kostenis, E., Felder, C., Zhang, L., Brodkin, J., Grinberg, A., Sheng, H., and Wess, J. (1999). Pronounced pharmacologic deficits in M2 muscarinic acetylcholine receptor knockout mice. Proc. Natl. Acad. Sci. USA *96*, 1692–1697.

Gotoh, C., Hong, Y.H., Iga, T., Hishikawa, D., Suzuki, Y., Song, S.H., Choi, K.C., Adachi, T., Hirasawa, A., Tsujimoto, G., et al. (2007). The regulation of adipogenesis through GPR120. Biochem. Biophys. Res. Commun. *354*, 591–597.

He, W., Miao, F.J., Lin, D.C., Schwandner, R.T., Wang, Z., Gao, J., Chen, J.L., Tian, H., and Ling, L. (2004). Citric acid cycle intermediates as ligands for orphan G-protein-coupled receptors. Nature *429*, 188–193.

Hill, C.A., Fox, A.N., Pitts, R.J., Kent, L.B., Tan, P.L., Chrystal, M.A., Cravchik, A., Collins, F.H., Robertson, H.M., and Zwiebel, L.J. (2002). G protein-coupled receptors in Anopheles gambiae. Science *298*, 176–178.

Ho, C., Conner, D.A., Pollak, M.R., Ladd, D.J., Kifor, O., Warren, H.B., Brown, E.M., Seidman, J.G., and Seidman, C.E. (1995). A mouse model of human familial hypocalciuric hypercalcemia and neonatal severe hyperparathyroidism. Nat. Genet. *11*, 389–394.

Hochachka, P.W., and Dressendorfer, R.H. (1976). Succinate accumulation in man during exercise. Eur. J. Appl. Physiol. Occup. Physiol. *35*, 235–242.

Hopkins, A.L., and Groom, C.R. (2002). The druggable genome. Nat. Rev. Drug Discov. *1*, 727–730.

Humbles, A.A., Lloyd, C.M., McMillan, S.J., Friend, D.S., Xanthou, G., McKenna, E.E., Ghiran, S., Gerard, N.P., Yu, C., Orkin, S.H., et al. (2004). A critical role for eosinophils in allergic airways remodeling. Science *305*, 1776–1779.

Incerti, B., Cortese, K., Pizzigoni, A., Surace, E.M., Varani, S., Coppola, M., Jeffery, G., Seeliger, M., Jaissle, G., Bennett, D.C., et al. (2000). Oa1 knockout: New insights on the pathogenesis of ocular albinism type 1. Hum. Mol. Genet. *9*, 2781–2788.

Ito, M., Oliverio, M.I., Mannon, P.J., Best, C.F., Maeda, N., Smithies, O., and Coffman, T.M. (1995). Regulation of blood pressure by the type 1A angiotensin II receptor gene. Proc. Natl. Acad. Sci. USA *92*, 3521–3525.

Jones, K.A., Borowsky, B., Tamm, J.A., Craig, D.A., Durkin, M.M., Dai, M., Yao, W.J., Johnson, M., Gunwaldsen, C., Huang, L.Y., et al. (1998). GABA(B) receptors function as a heteromeric assembly of the subunits GABA(B)R1 and GABA(B)R2. Nature *396*, 674–679.

Joost, P., and Methner, A. (2002). Phylogenetic analysis of 277 human G-protein-coupled receptors as a tool for the prediction of orphan receptor ligands. Genome Biol. *3*, RESEARCH0063.

Karsak, M., Gaffal, E., Date, R., Wang-Eckhardt, L., Rehnelt, J., Petrosino, S., Starowicz, K., Steuder, R., Schlicker, E., Cravatt, B., et al. (2007). Attenuation of allergic contact dermatitis through the endocannabinoid system. Science *316*, 1494–1497.

Kaupmann, K., Malitschek, B., Schuler, V., Heid, J., Froestl, W., Beck, P., Mosbacher, J., Bischoff, S., Kulik, A., Shigemoto, R., et al. (1998). GABA(B)-receptor subtypes assemble into functional heteromeric complexes. Nature *396*, 683–687.

Kelly, M.A., Rubinstein, M., Asa, S.L., Zhang, G., Saez, C., Bunzow, J.R., Allen, R.G., Hnasko, R., Ben-Jonathan, N., Grandy, D.K., et al. (1997). Pituitary lactotroph hyperplasia and chronic hyperprolactinemia in dopamine D2 receptor-deficient mice. Neuron *19*, 103–113.

Kim, C.H., Kunkel, E.J., Boisvert, J., Johnston, B., Campbell, J.J., Genovese, M.C., Greenberg, H.B., and Butcher, E.C. (2001). Bonzo/CXCR6 expression defines type 1-polarized T-cell subsets with extralymphoid tissue homing potential. J. Clin. Invest. *107*, 595–601.

Krebs, H.A. (1950). Chemical composition of blood plasma and serum. Annu. Rev. Biochem. *19*, 409–430.

Krogan, N.J., Cagney, G., Yu, H., Zhong, G., Guo, X., Ignatchenko, A., Li, J., Pu, S., Datta, N., Tikuisis, A.P., et al. (2006). Global landscape of protein complexes in the yeast Saccharomyces cerevisiae. Nature *440*, 637–643.

Kumar, U., Laird, D., Srikant, C.B., Escher, E., and Patel, Y.C. (1997). Expression of the five somatostatin receptor (SSTR1–5) subtypes in rat pituitary somatotrophes: Quantitative analysis by double-layer immunofluorescence confocal microscopy. Endocrinology *138*, 4473–4476.

Kuner, R., Kohr, G., Grunewald, S., Eisenhardt, G., Bach, A., and Kornau, H.C. (1999). Role of heteromer formation in GABAB receptor function. Science *283*, 74–77.

Kushnir, M.M., Komaromy-Hiller, G., Shushan, B., Urry, F.M., and Roberts, W.L. (2001). Analysis of dicarboxylic acids by tandem mass spectrometry. High-throughput quantitative measurement of methylmalonic acid in serum, plasma, and urine. Clin. Chem. *47*, 1993–2002.

Le, L.Q., Kabarowski, J.H., Weng, Z., Satterthwaite, A.B., Harvill, E.T., Jensen, E.R., Miller, J.F., and Witte, O.N. (2001). Mice lacking the orphan G protein-coupled receptor G2A develop a late-onset autoimmune syndrome. Immunity *14*, 561–571.

Liberles, S.D., and Buck, L.B. (2006). A second class of chemosensory receptors in the olfactory epithelium. Nature *442*, 645–650.

Lin, S.C., Lin, C.R., Gukovsky, I., Lusis, A.J., Sawchenko, P.E., and Rosenfeld, M.G. (1993). Molecular basis of the little mouse phenotype and implications for cell type-specific growth. Nature *364*, 208–213.

Lindemann, L., Meyer, C.A., Jeanneau, K., Bradaia, A., Ozmen, L., Bluethmann, H., Bettler, B., Wettstein, J.G., Borroni, E., Moreau, J.L., et al. (2008). Trace amine-associated receptor 1 modulates dopaminergic activity. J. Pharmacol. Exp. Ther. *324*, 948–956.

Liu, Y., Wada, R., Yamashita, T., Mi, Y., Deng, C.X., Hobson, J.P., Rosenfeldt, H.M., Nava, V.E., Chae, S.S., Lee, M.J., et al. (2000). Edg-1, the G protein-coupled receptor for sphingosine-1-phosphate, is essential for vascular maturation. J. Clin. Invest. *106*, 951–961.

Lorsignol, A., Vande Vijver, V., Ramaekers, D., Vankelecom, H., and Denef, C. (1999). Detection of melanocortin-3 receptor mRNA in immature rat pituitary: Functional relation to gamma3-MSH-induced changes in intracellular Ca2+ concentration? J. Neuroendocrinol. *11*, 171–179.

Lovenberg, T.W., Baron, B.M., de Lecea, L., Miller, J.D., Prosser, R.A., Rea, M.A., Foye, P.E., Racke, M., Slone, A.L., Siegel, B.W., et al. (1993). A novel adenylyl cyclase-activating serotonin receptor (5–HT7) implicated in the regulation of mammalian circadian rhythms. Neuron *11*, 449–458.

Malone, M.H., Wang, Z., and Distelhorst, C.W. (2004). The glucocorticoid-induced gene tdag8 encodes a pro-apoptotic G protein-coupled receptor whose activation promotes glucocorticoid-induced apoptosis. J. Biol. Chem. *279*, 52850–52859.

Marsh, D.J., Hollopeter, G., Kafer, K.E., and Palmiter, R.D. (1998). Role of the Y5 neuropeptide Y receptor in feeding and obesity. Nat. Med. *4*, 718–721.

Mazella, J., Botto, J.M., Guillemare, E., Coppola, T., Sarret, P., and Vincent, J.P. (1996). Structure, functional expression, and cerebral localization of the levocabastine-sensitive neurotensin/neuromedin N receptor from mouse brain. J. Neurosci. *16*, 5613–5620.

McGee, J., Goodyear, R.J., McMillan, D.R., Stauffer, E.A., Holt, J.R., Locke, K.G., Birch, D.G., Legan, P.K., White, P.C., Walsh, E.J., et al. (2006). The very large G-protein-coupled receptor VLGR1: A component of the ankle

link complex required for the normal development of auditory hair bundles. J. Neurosci. *26*, 6543–6553.

Moreno, F.J., Mills, I., Garcia-Sainz, J.A., and Fain, J.N. (1983). Effects of pertussis toxin treatment on the metabolism of rat adipocytes. J. Biol. Chem. *258*, 10938–10943.

Moskowitz, J., and Fain, J.N. (1969). Hormonal regulation of lipolysis and phosphorylase activity in human fat cells. J. Clin. Invest. *48*, 1802–1808.

Muller, G. (2000). Towards 3D structures of G protein-coupled receptors: A multidisciplinary approach. Curr. Med. Chem. *7*, 861–888.

Nagasawa, T., Hirota, S., Tachibana, K., Takakura, N., Nishikawa, S., Kitamura, Y., Yoshida, N., Kikutani, H., and Kishimoto, T. (1996). Defects of B-cell lymphopoiesis and bone-marrow myelopoiesis in mice lacking the CXC chemokine PBSF/SDF-1. Nature *382*, 635–638.

Nathans, J., and Hogness, D.S. (1983). Isolation, sequence analysis, and intron-exon arrangement of the gene encoding bovine rhodopsin. Cell *34*, 807–814.

Nordmann, J., and Nordmann, R. (1961). Organic acids in blood and urine. Adv. Clin. Chem. *4*, 53–120.

Peirson, S.N., Butler, J.N., and Foster, R.G. (2003). Experimental validation of novel and conventional approaches to quantitative real-time PCR data analysis. Nucleic Acids Res. *31*, e73.

Popova, N.K., Naumenko, V.S., and Plyusnina, I.Z. (2007). Involvement of brain serotonin 5–HT1A receptors in genetic predisposition to aggressive behavior. Neurosci. Behav. Physiol. *37*, 631–635.

Rao, S., Garrett-Sinha, L.A., Yoon, J., and Simon, M.C. (1999). The Ets factors PU.1 and Spi-B regulate the transcription in vivo of P2Y10, a lymphoid restricted heptahelical receptor. J. Biol. Chem. *274*, 34245–34252.

Regard, J.B., Kataoka, H., Cano, D.A., Camerer, E., Yin, L., Zheng, Y.W., Scanlan, T.S., Hebrok, M., and Coughlin, S.R. (2007). Probing cell type-specific functions of G(i) in vivo identifies GPCR regulators of insulin secretion. J. Clin. Invest. *117*, 4034–4043.

Rodbell, M. (1964). Metabolism of isolated fat cells. I. Effects of hormones on hlucose metabolism and lipolysis. J. Biol. Chem. *239*, 375–380.

Sadagopan, N., Li, W., Roberds, S.L., Major, T., Preston, G.M., Yu, Y., and Tones, M.A. (2007). Circulating succinate is elevated in rodent models of hypertension and metabolic disease. Am. J. Hypertens. *20*, 1209–1215.

Saiardi, A., Bozzi, Y., Baik, J.H., and Borrelli, E. (1997). Antiproliferative role of dopamine: Loss of D2 receptors causes hormonal dysfunction and pituitary hyperplasia. Neuron *19*, 115–126.

Saldanha, A.J. (2004). Java Treeview–extensible visualization of microarray data. Bioinformatics *20*, 3246–3248.

Schuldiner, M., Collins, S.R., Thompson, N.J., Denic, V., Bhamidipati, A., Punna, T., Ihmels, J., Andrews, B., Boone, C., Greenblatt, J.F., et al. (2005). Exploration of the function and organization of the yeast early secretory pathway through an epistatic miniarray profile. Cell *123*, 507–519.

Scrocchi, L.A., Brown, T.J., MaClusky, N., Brubaker, P.L., Auerbach, A.B., Joyner, A.L., and Drucker, D.J. (1996). Glucose intolerance but normal satiety in mice with a null mutation in the glucagon-like peptide 1 receptor gene. Nat. Med. *2*, 1254–1258.

Segre, D., Deluna, A., Church, G.M., and Kishony, R. (2005). Modular epistasis in yeast metabolism. Nat. Genet. *37*, 77–83.

Shuster, D.E., Kehrli, M.E., Jr., and Ackermann, M.R. (1995). Neutrophilia in mice that lack the murine IL-8 receptor homolog. Science *269*, 1590–1591.

Simonin, F., Gaveriaux-Ruff, C., Befort, K., Matthes, H., Lannes, B., Micheletti, G., Mattei, M.G., Charron, G., Bloch, B., and Kieffer, B. (1995). kappa-Opioid receptor in humans: cDNA and genomic cloning, chromosomal assignment, functional expression, pharmacology, and expression pattern in the central nervous system. Proc. Natl. Acad. Sci. USA *92*, 7006–7010.

Sinha, T.K., Thajchayapong, P., Queener, S.F., Allen, D.O., and Bell, N.H. (1976). On the lipolytic action of parathyroid hormone in man. Metabolism *25*, 251–260.

Soga, T., Kamohara, M., Takasaki, J., Matsumoto, S., Saito, T., Ohishi, T., Hiyama, H., Matsuo, A., Matsushime, H., and Furuichi, K. (2003). Molecular identification of nicotinic acid receptor. Biochem. Biophys. Res. Commun. *303*, 364–369.

Soto, H., Wang, W., Strieter, R.M., Copeland, N.G., Gilbert, D.J., Jenkins, N.A., Hedrick, J., and Zlotnik, A. (1998). The CC chemokine 6Ckine binds the CXC chemokine receptor CXCR3. Proc. Natl. Acad. Sci. USA *95*, 8205–8210.

Stacey, M., Chang, G.W., Sanos, S.L., Chittenden, L.R., Stubbs, L., Gordon, S., and Lin, H.H. (2002). EMR4, a novel epidermal growth factor (EGF)-TM7 molecule up-regulated in activated mouse macrophages, binds to a putative cellular ligand on B lymphoma cell line A20. J. Biol. Chem. *277*, 29283–29293.

Sugaya, T., Nishimatsu, S., Tanimoto, K., Takimoto, E., Yamagishi, T., Imamura, K., Goto, S., Imaizumi, K., Hisada, Y., Otsuka, A., et al. (1995). Angiotensin II type 1a receptor-deficient mice with hypotension and hyperreninemia. J. Biol. Chem. *270*, 18719–18722.

Sun, H., Gilbert, D.J., Copeland, N.G., Jenkins, N.A., and Nathans, J. (1997a). Peropsin, a novel visual pigment-like protein located in the apical microvilli of the retinal pigment epithelium. Proc. Natl. Acad. Sci. USA *94*, 9893–9898.

Sun, H., Macke, J.P., and Nathans, J. (1997b). Mechanisms of spectral tuning in the mouse green cone pigment. Proc. Natl. Acad. Sci. USA *94*, 8860–8865.

Susulic, V.S., Frederich, R.C., Lawitts, J., Tozzo, E., Kahn, B.B., Harper, M.E., Himms-Hagen, J., Flier, J.S., and Lowell, B.B. (1995). Targeted disruption of the beta 3-adrenergic receptor gene. J. Biol. Chem. *270*, 29483–29492.

Tsutsumi, M., Zhou, W., Millar, R.P., Mellon, P.L., Roberts, J.L., Flanagan, C.A., Dong, K., Gillo, B., and Sealfon, S.C. (1992). Cloning and functional expression of a mouse gonadotropin-releasing hormone receptor. Mol. Endocrinol. *6*, 1163–1169.

Tunaru, S., Kero, J., Schaub, A., Wufka, C., Blaukat, A., Pfeffer, K., and Offermanns, S. (2003). PUMA-G and HM74 are receptors for nicotinic acid and mediate its anti-lipolytic effect. Nat. Med. *9*, 352–355.

Valet, P., Pages, C., Jeanneton, O., Daviaud, D., Barbe, P., Record, M., Saulnier-Blache, J.S., and Lafontan, M. (1998). Alpha2-adrenergic receptor-mediated release of lysophosphatidic acid by adipocytes. A paracrine signal for preadipocyte growth. J. Clin. Invest. *101*, 1431–1438.

Varona, R., Villares, R., Carramolino, L., Goya, I., Zaballos, A., Gutierrez, J., Torres, M., Martinez, A.C., and Marquez, G. (2001). CCR6-deficient mice have impaired leukocyte homeostasis and altered contact hypersensitivity and delayed-type hypersensitivity responses. J. Clin. Invest. *107*, R37–R45.

Vassilatis, D.K., Hohmann, J.G., Zeng, H., Li, F., Ranchalis, J.E., Mortrud, M.T., Brown, A., Rodriguez, S.S., Weller, J.R., Wright, A.C., et al. (2003). The G protein-coupled receptor repertoires of human and mouse. Proc. Natl. Acad. Sci. USA *100*, 4903–4908.

White, J.H., Wise, A., Main, M.J., Green, A., Fraser, N.J., Disney, G.H., Barnes, A.A., Emson, P., Foord, S.M., and Marshall, F.H. (1998). Heterodimerization is required for the formation of a functional GABA(B) receptor. Nature *396*, 679–682.

Willie, J.T., Chemelli, R.M., Sinton, C.M., Tokita, S., Williams, S.C., Kisanuki, Y.Y., Marcus, J.N., Lee, C., Elmquist, J.K., Kohlmeier, K.A., et al. (2003). Distinct narcolepsy syndromes in Orexin receptor-2 and Orexin null mice: Molecular genetic dissection of Non-REM and REM sleep regulatory processes. Neuron *38*, 715–730.

Wise, A., Foord, S.M., Fraser, N.J., Barnes, A.A., Elshourbagy, N., Eilert, M., Ignar, D.M., Murdock, P.R., Steplewski, K., Green, A., et al. (2003). Molecular identification of high and low affinity receptors for nicotinic acid. J. Biol. Chem. *278*, 9869–9874.

Wurbel, M.A., Malissen, M., Guy-Grand, D., Meffre, E., Nussenzweig, M.C., Richelme, M., Carrier, A., and Malissen, B. (2001). Mice lacking the CCR9 CC-chemokine receptor show a mild impairment of early T- and B-cell development and a reduction in T-cell receptor gammadelta(+) gut intraepithelial lymphocytes. Blood *98*, 2626–2632.